

# Constraints on a $f(R)$ gravity dark energy model with early scaling evolution

Chan-Gyung Park<sup>1</sup>, Jai-chan Hwang<sup>1</sup>, and Hyerim Noh<sup>2</sup>

<sup>1</sup>*Department of Astronomy and Atmospheric Sciences, Kyungpook National University, Taegu, Korea*

<sup>2</sup>*Korea Astronomy and Space Science Institute, Daejeon, Korea*

The modified gravity with  $f(R) = R^{1+\epsilon}$  ( $\epsilon > 0$ ) allows a scaling solution where the density of gravity sector follows the density of the dominant fluid. We present initial conditions of background and perturbation variables during the scaling evolution regime in the modified gravity. As a possible dark energy model we consider a gravity with a form  $f(R) = R^{1+\epsilon} + qR^{-n}$  ( $-1 < n \leq 0$ ) where the second term drives the late-time acceleration. We show that our  $f(R)$  gravity parameters are very sensitive to the baryon perturbation growth and baryon density power spectrum, and present observational constraints on the model parameters. Our analysis suggests that only the parameter space extremely close to the  $\Lambda$ CDM model is allowed.

PACS numbers: 98.80.-k, 95.36.+x

## I. INTRODUCTION

The current accelerated expansion of the universe has been theoretically explained by either the cosmological constant or some kind of dynamical dark energy in the context of field or modified gravity (see Ref. [1] for recent reviews).

In the modified gravity such as  $f(R)$  gravity [2] (see Refs. [3] for reviews and [4–14] for recent works), background evolution sometimes confronts with a numerical difficulty. The background evolution is not easily handled numerically during the early radiation dominated era in the modified gravity with a functional form  $f(R) = R + f_{\text{DE}}(R)$ , where  $f_{\text{DE}}$  drives the late-time acceleration. The cosmologically viable forms of  $f_{\text{DE}}$  proposed so far are  $qR^{-n}$  [5–7] and forms given by Hu & Sawicki [8], Starobinsky [9], and so on [10, 11]. In all models, the second term  $f_{\text{DE}}$  becomes extremely subdominant compared with  $R$  in the early radiation dominated era so that the  $f(R)$  gravity effectively goes over into the Einstein gravity; in general, however, the evolution could be more complicated, see [12]. Since the quantity  $F \equiv df/dR$  becomes extremely close to unity in such a situation, evolving a differential equation like Eq. (1) or (2) below is sometimes not numerically feasible.

Adopting the modified form  $f(R) = R^{1+\epsilon} + f_{\text{DE}}$  with small positive  $\epsilon$  together with appropriate initial conditions we can evade this numerical problem (here we use the Planck unit with  $8\pi G \equiv 1 \equiv c$ ). It is known that the first term  $R^{1+\epsilon}$  which is dominant in the early epoch allows the density of gravity sector to follow that of dominant fluid (scaling evolution) [5].

We are motivated to study the case in order to investigate the observationally allowed regions with qualitatively different evolution available in our case of  $f(R)$  gravity. By considering  $R^{1+\epsilon}$  term, however, the gravity with  $f_{\text{DE}} = -2\Lambda$  does not go over into the Einstein gravity in recent era. We will still consider values of  $\epsilon$  which is likely to be excluded by the solar-system test because with vanishingly small  $\epsilon$  the system of equations

cannot be handled numerically due to limited numerical precision in the early era. Though, we will show that for smallest value of  $\epsilon$  we considered, the cosmological evolution we study is numerically similar to the evolution in Einstein's gravity with cosmological constant.

In this paper, we present initial conditions of background and perturbed variables during the scaling regime in this gravity. Using the initial conditions for scaling evolution we present background evolution, matter (density) and cosmic microwave background (CMB) anisotropy power spectra, and perturbation growth in the gravity with  $f_{\text{DE}} = qR^{-n}$ . We show that the CMB power spectrum is not sensitive to the model parameters, and explore the viable parameter space constrained by the type Ia supernova (SNIa), matter power spectrum, and the future perturbation growth factor observation.

Throughout this paper we assume spatial flatness ( $K \equiv 0$ ). Notations and the basic set of equations in  $f(R)$  gravity are summarized in Ref. [15].

## II. BACKGROUND AND PERTURBATION EQUATIONS

The background evolution in the  $f(R)$  gravity is described by (see Eqs. (43), (57) and (59) of Ref. [15])

$$\ddot{F} + 3H\dot{F} + \frac{1}{3}(2f - FR) = \frac{1}{3}(\mu_m - 3p_m), \quad (1)$$

where  $H \equiv \dot{a}/a$ ,  $a(t)$  is the cosmic scale factor, a dot represents a derivative with respect to the cosmic time  $t$ , and  $\mu_m$  and  $p_m$  are collective density and pressure for radiation ( $R$ ) and matter ( $M$ ):  $\mu_m = \mu_R + \mu_M$  and likewise for  $p_m$ . Using  $\dot{F} = F_{,R}\dot{R}$  with  $F_{,R} \equiv dF/dR$ , Eq. (1) is transformed into a differential equation for  $R$

$$\ddot{R} + \frac{F_{,RR}}{F_{,R}}\dot{R}^2 + 3H\dot{R} + \frac{2f - RF}{3F_{,R}} = \frac{1}{3F_{,R}}(\mu_m - 3p_m), \quad (2)$$

which is what we actually solved numerically. To evolve this equation we need  $H(t)$ . For spatially flat Robertson-

Walker metric, we have (see Eqs. (43) and (57) of Ref. [15])

$$H^2 = \frac{1}{3F} (\mu_m + F\mu_X), \quad F\mu_X \equiv \frac{1}{2}(FR - f) - 3H\dot{F}, \quad (3)$$

where  $\mu_X$  indicates the energy density of  $f(R)$  gravity sector (hereafter  $X$ -component), and  $R = 6(2H^2 + \dot{H})$ . With the definition of conventional density parameters,  $\Omega_i = \mu_i/(3H^2)$  ( $i = R, M, X$ ), we have a relation  $(\Omega_R + \Omega_M)/F + \Omega_X = 1$  from Eq. (3). The equation of state of the  $X$ -component is defined as  $w_X \equiv p_X/\mu_X$ , where

$p_X$  is the pressure of the  $X$ -component given by (see Eq. (57) of Ref. [15])

$$Fp_X \equiv -\frac{1}{2}(FR - f) + \ddot{F} + 2H\dot{F}. \quad (4)$$

The perturbation equations in the CDM-comoving gauge (CCG), which sets perturbed velocity of cold dark matter is set to zero ( $v_c \equiv 0$ ) as the temporal gauge (hypersurface) condition, are presented in Eqs. (86)–(88), (66), and (67) of Ref. [15]. Using  $\delta R$  as the perturbation variable, we have

$$\begin{aligned} \left(\frac{\delta R}{R}\right)'' + \left(3 + \frac{\dot{H}}{H^2} + 2\frac{F_{,RR}}{F_{,R}}R' + 2\frac{R'}{R}\right) \left(\frac{\delta R}{R}\right)' + \left\{\frac{F}{3H^2F_{,R}} - \frac{R}{3H^2} + \frac{F_{,RR}}{F_{,R}} \left[R'' + \left(3 + \frac{\dot{H}}{H^2}\right)R'\right] \right. \\ \left. + \frac{F_{,RRR}}{F_{,R}}R'^2 + \frac{R''}{R} + \frac{R'}{R} \left(3 + \frac{\dot{H}}{H^2} + 2\frac{F_{,RR}}{F_{,R}}R'\right) + \frac{k^2}{a^2H^2}\right\} \left(\frac{\delta R}{R}\right) = \frac{R'}{R} \left(\frac{\kappa}{H}\right) + \frac{1}{3H^2F_{,R}R} (\delta\mu_m - 3\delta p_m), \quad (5) \end{aligned}$$

$$\begin{aligned} \left(\frac{\kappa}{H}\right)' + \left(2 + \frac{\dot{H}}{H^2} - \frac{F_{,R}}{F}R'\right) \left(\frac{\kappa}{H}\right) = -3\frac{F_{,R}}{F}R \left[\left(\frac{\delta R}{R}\right)' \right. \\ \left. + \left(-\frac{f}{6H^2F} + \frac{\mu_m}{3H^2F} + \frac{F}{6H^2F_{,R}} - \frac{F_{,R}}{F}R' + \frac{F_{,RR}}{F_{,R}}R' + \frac{R'}{R} + \frac{1}{3}\frac{k^2}{a^2H^2}\right) \left(\frac{\delta R}{R}\right)\right] + \frac{1}{H^2F}\delta\mu_m, \quad (6) \end{aligned}$$

$$\delta'_c = \frac{\kappa}{H}, \quad (7)$$

$$\delta'_w = (1+w) \left(\frac{\kappa}{H} - \frac{k}{aH}v_w\right), \quad (8)$$

$$v'_w + (1-3w)v_w = \frac{w}{1+w} \frac{k}{aH}\delta_w, \quad (9)$$

where  $\delta\mu_m$  and  $\delta p_m$  are collective perturbed density, pressure, respectively. In our full numerical treatment the collective fluids includes the CDM, baryon, radiation (photons and neutrinos), etc; the radiation parts include photons handled by Boltzmann equations or tight coupling approximation. In Eqs. (8) and (9), as an example, we present a fluid with a constant equation of state parameter  $w \equiv p_w/\mu_w$ ;  $\delta_w = \delta\mu_w/\mu_w$  is the density contrast and  $v_w$  is the perturbed velocity of the dominant fluid. Here a prime indicates a derivative with respect to  $\ln a$  ( $F' \equiv dF/d\ln a$ ),  $k$  is the comoving wave number, and  $\kappa$  is the perturbed expansion of normal frame vector. As we consider the CCG we need to include the CDM component even in the case it is subdominant. In case it is subdominant, we have at least a sixth order differential equation as presented in Eqs. (5)–(9).

### III. INITIAL CONDITIONS FOR SCALING EVOLUTION

In the early era, let us consider a functional form

$$f(R) = \alpha R^{1+\epsilon}, \quad (10)$$

where  $\epsilon$  is small positive constant; for generality we introduced a coefficient  $\alpha$  which is unity in our unit. The gravity of pure power-law form allows scaling evolution in which the density of  $X$ -component follows that of the dominant fluid [5], and the corresponding potential in the Einstein frame is a pure exponential potential [13]. Here we put an ansatz that  $F\mu_X$  evolves as the dominant ideal fluid with constant equation of state ( $w = p_w/\mu_w = \delta p_w/\delta\mu_w$ ) as

$$F\mu_X = \frac{1}{2}(FR - f) - 3H\dot{F} \equiv A\mu_w, \quad (11)$$

where  $A$  is the constant density fraction of  $X$ -component relative to the dominant fluid. By combining Eqs. (1), (3), and (11), we can derive

$$3FR - f = 2\mu_w[(1-3w) + (2-3w)A], \quad (12)$$

$$\frac{F'}{F} = \frac{(1-3w)[(1+A)f - FR] + A(1+3w)FR}{(1+A)(f - 3FR)}. \quad (13)$$

Equations (12) and (13) provide the scaling initial conditions for  $F$  and  $F'$ , respectively. Noting that  $3FR - f \propto$

$a^{-3(1+w)}$  in Eq. (12) and specifying the form of  $f(R)$  in Eq. (10), we obtain an exact expression for  $R$

$$R = H_0^2 \left[ \frac{6\Omega_{w0}[(1-3w) + (2-3w)A]}{\alpha(2+3\epsilon)(a/a_0)^{3(1+w)}} \right]^{\frac{1}{1+\epsilon}}, \quad (14)$$

and its time derivative

$$R' = -3\frac{1+w}{1+\epsilon}R, \quad (15)$$

where  $\Omega_{w0} = \mu_{w0}/(3H_0^2)$  is the density parameter of  $w$ -fluid at the present epoch (indicated by the subscript 0). Inserting Eq. (15) into Eq. (13), we determine

$$A = \frac{\epsilon(7+10\epsilon) + 3\epsilon(1+2\epsilon)w}{2-3\epsilon-8\epsilon^2-3\epsilon(1+2\epsilon)w}. \quad (16)$$

Equations (14)–(16) can be used as initial conditions for the scaling density evolution of  $X$ -component in the  $f(R) = R^{1+\epsilon}$  gravity. The scaling behavior is possible for general constant  $w$  value of the dominant fluid. As we set the scaling initial condition, the density of  $X$ -component follows (scales) the dominant fluid component even for changing  $w$  value of the dominant component; for example, from radiation dominated era to the matter dominated era.

Now, for the perturbed initial conditions, applying the same method used in Ref. [16] that presents initial conditions of perturbed variables during the scaling regime of the cosmology based on a minimally coupled scalar field, we find initial conditions of perturbed variables in our  $f(R)$  gravity. In the large-scale limit ( $\frac{k}{aH} \rightarrow 0$ ), with the help of Eqs. (3), (10)–(16), all the background-related coefficients in Eqs. (5)–(9) are expressed in terms of  $\epsilon$  and  $w$  alone during the scaling regime. We have solutions for Eqs. (5)–(9) in the form

$$\delta_w \propto \frac{\delta R}{R} \propto e^{n \ln a}, \quad (17)$$

where

$$n = \frac{1-2\epsilon+3w}{1+\epsilon}, \quad -\frac{3}{2} \left( \frac{1+w}{1+\epsilon} \right), \quad (18)$$

$$\frac{1}{4\epsilon(1+\epsilon)} \left\{ -3\epsilon + 3\epsilon(1+2\epsilon)w \pm \left[ -16\epsilon - 31\epsilon^2 + 160\epsilon^3 + 256\epsilon^4 + 3\epsilon(16-22\epsilon - 28\epsilon^2 + 64\epsilon^3)w - 9\epsilon^2(7+12\epsilon-4\epsilon^2)w^2 \right]^{\frac{1}{2}} \right\}.$$

The solutions have been obtained by MAPLE software of version 11 [17]. By choosing the first one as the growing mode solution, we get initial conditions of the perturbed

variables,

$$\delta_w = Ce^{\frac{1-2\epsilon+3w}{1+\epsilon} \ln a}, \quad \left( \frac{\kappa}{H} \right) = \frac{1-2\epsilon+3w}{(1+\epsilon)(1+w)}\delta_w, \quad (19)$$

$$\frac{\delta R}{R} = \frac{1-4\epsilon-3(1+2\epsilon)w}{1+7\epsilon-12\epsilon^2-3(1-\epsilon)(1-2\epsilon)w}\delta_w, \quad \left( \frac{\delta R}{R} \right)' = \frac{1-2\epsilon+3w}{1+\epsilon} \left( \frac{\delta R}{R} \right),$$

where  $C$  is the initial amplitude.

Solutions similar to Eq. (18) were presented in Ref. [14]. Compared with the solutions in Ref. [14] which were based on the comoving gauge of the dominant fluid (the  $w$ -fluid), our solutions are based on the CCG gauge condition which is the CDM comoving gauge. A comparison of the two results shows that the growing solution coincides and the other three solutions differ for  $w \neq 0$ . We are interested only in the growing solution, and the solutions in Eq. (19) coincide with the one in Ref. [14].

#### IV. A DARK ENERGY MODEL AND CONSTRAINTS

In this section, we present numerical evolution of background and perturbed quantities in a dark energy model based on the  $f(R)$  gravity with early scaling era. We consider a gravity with a form

$$f(R) = R^{1+\epsilon} + qR^{-n}, \quad (20)$$

where  $\epsilon > 0$  and  $-1 < n \leq 0$ . Our model allows exact scaling during the radiation and matter dominated eras (provided by the first term) and drives the late-time acceleration in the recent epoch (provided by the second term). Our model with the scaling initial conditions does not cause the numerical problem discussed in Sec. I. In the early radiation dominated epoch (e.g., starting from  $a_i/a_0 = 10^{-11}$  in this paper), for small  $\epsilon = 10^{-8} \sim 10^{-6}$  the quantity  $F \simeq (1+\epsilon)R^\epsilon$  evolves with values slightly larger than unity so that Eq. (1) or (2) can be numerically manageable within the precision of usual computing environment. The evolution of both background and perturbed variables becomes numerically unstable as  $\epsilon$  gets smaller (e.g.,  $\epsilon \lesssim 10^{-9}$  for  $a_i/a_0 = 10^{-11}$ ). This is because at the early epoch the quantity  $F$  is so close to the unity that the time-variation of  $F$  is not numerically manageable even in double precision accuracy.

Although the detailed study is not given here, the value of  $\epsilon$  can be more tightly constrained by the solar system test. For example, according to the criterion given by Ref. [28], one expect  $\epsilon \lesssim 10^{-17}$  for  $R/H_0^2 = 10^5$ . As we explained earlier, such a small value of  $\epsilon$  is numerically problematic in the early era due to limited numerical precision currently available. Thus although the values of  $\epsilon$  we consider are likely to be too large considering the solar-system constraint, as shown below, the case of  $\epsilon = 10^{-7}$  and  $n = 0$  gives power spectra and perturbation

growth that are observationally indistinguishable from the predictions of the  $\Lambda$ CDM model in Einstein gravity ( $\epsilon = 0, n = 0$ ).

There is one numerical task needed during the background evolution of  $f(R)$  gravity. Evolving Eq. (1) or (2) demands a fine-tuning process to satisfy the condition that the normalized Hubble parameter at the present epoch should be equal to unity,  $\hat{H}_0 = 1$ , where  $\hat{H} \equiv H/H_0$ . When the radiation and the matter energy densities at the present epoch are fixed, one of the coefficients appearing in the  $f(R)$  functional form should be adjusted to match this condition for given initial conditions of  $R$  and  $R'$ , or vice versa. In our case we adjust  $q$  appearing in Eq. (20) to satisfy  $\hat{H}_0 = 1$  for a given set of scaling initial conditions. The same numerical situation also appears in the Einstein gravity with dark energy model based on a minimally coupled scalar field.

In a modified gravity with the form  $f(R) = R + qR^{-n}$ , the method of imposing initial conditions for the background evolution used in the literature is unclear to us. Furthermore, the coefficient  $q$  is not single-valued depending on the choice of  $n$  and initial conditions of  $R$  and  $R'$ . In an extreme case when  $n = -0.97$ ,  $R_i = 10^{-5}H_0^2$ , and  $R'_i = 0$  at  $a_i/a_0 = 10^{-11}$  with other parameters fixed with the Wilkinson Microwave Anisotropy Probe (WMAP) 7-year best-fit parameters (see below), there are nine multiple values of  $q$  satisfying  $\hat{H}_0 = 1$  in the range  $-0.7222 < q/H_0^{2n+2} < 0$ . Under the same (non-scaling) condition, multiple  $q$  values are also obtained in our  $f(R)$  gravity. On the other hand, our initial conditions for the scaling evolution presented in Sec. III are exact and general so that they can be applied to any dominant fluid with a constant equation of state  $w$ . With the scaling initial conditions,  $q$  is single-valued over the whole range of  $n$  considered.

In our analysis we considered cases where the behavior of our  $f(R)$  gravity, Eq. (20) can be approximated by the first term ( $R^{1+\epsilon}$ ; higher power of  $R$ ) at early times and is dominated by the second term ( $qR^{-n}$ ,  $-1 < n \leq 0$ ; lower power of  $R$ ) at late time during the acceleration phase. However, it should be emphasized that the assumption that the higher power of  $R$  should dominate at early epoch and the lower power of  $R$  should dominate at later epoch is not necessarily the case due to the nonlinearities of the  $f(R)$  gravity theory [12]. Because the scaling background evolution guaranteed by the scaling initial condition leads to decreasing  $R$  value in time for  $w > -1$  [this follows from Eq. (14)], this allows the transition from higher to lower  $R$ -power regimes in our case.

Figure 1 shows background evolution of our  $f(R)$  gravity with  $\epsilon = 0.001$  and varying  $n$  (color solid curves). The background parameters shown are density parameters  $\Omega_i$ , energy densities  $\mu_i$ , equation of state  $w_X$ , relative Hubble parameter ( $H/H_{\Lambda\text{CDM}}$ ) and distance modulus ( $\bar{\mu} - \bar{\mu}_{\Lambda\text{CDM}}$ ) with respect to the fiducial  $\Lambda$ CDM model. As a fiducial model we take a flat  $\Lambda$ CDM universe with parameters  $\Omega_{M0} = 0.274$  ( $\Omega_{c0} = 0.2284$  and

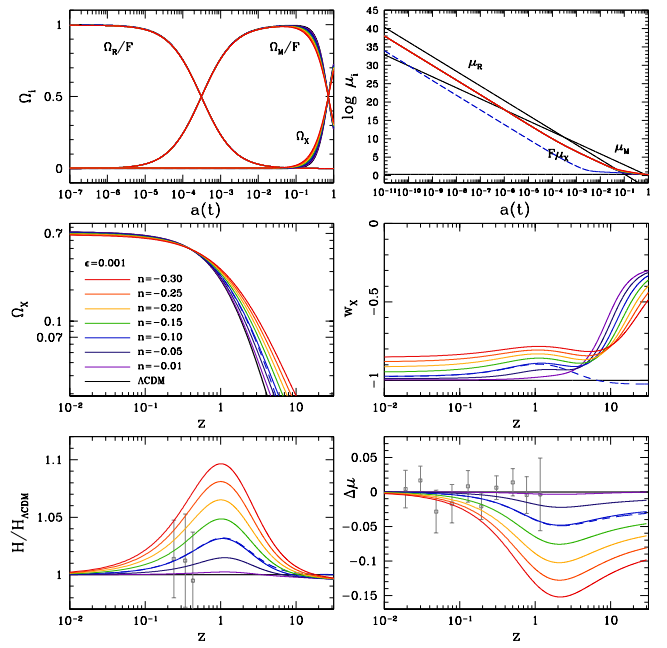


FIG. 1: Background evolution in the  $f(R) = R^{1+\epsilon} + qR^{-n}$  gravity with  $\epsilon = 0.001$  and varying  $n = -0.01, -0.05, -0.10, -0.15, -0.20, -0.25$ , and  $-0.30$  (color solid curves). Results for  $\epsilon = 10^{-7}$  and  $n = -0.1$  are added with blue dashed curves. (Top panels) Evolution of  $\Omega_i$  and  $\mu_i$  as a function of scale factor  $a(t)$ , where  $i = R, M, X$  indicates radiation, matter (baryon plus CDM), and gravity sector, respectively. (Middle and bottom panels). Evolution of  $\Omega_X$ , equation of state of  $X$ -component  $w_X$ , Hubble parameter  $H/H_{\Lambda\text{CDM}}$ , and distance modulus  $\Delta\mu = \bar{\mu} - \bar{\mu}_{\Lambda\text{CDM}}$  relative to the  $\Lambda$ CDM model, where  $\bar{\mu}$  represents the distance modulus. In all panels  $\Lambda$ CDM predictions are shown as thick black curves. The Hubble parameter data is taken from Ref. [19], and the binned SNIa data points are from the UNION2 sample [20].

$\Omega_{b0} = 0.0456$ ),  $\Omega_{\Lambda0} = 0.7278$ ,  $h = 0.704$ ,  $n_s = 0.963$ ,  $\sigma_8 = 0.809$ ,  $T_0 = 2.725$  K,  $Y_{\text{He}} = 0.24$ ,  $N_\nu = 3.04$  with reionization optical depth  $\tau = 0.087$  based on the WMAP 7-year observations [18]. In all  $f(R)$  gravity models, we set  $\Omega_{X0} \equiv \Omega_{\Lambda0}$ . With the fiducial model parameters, the  $\epsilon$  has an upper bound  $\epsilon_{\text{BBN}} = 0.011314$  so that the initial contribution from the dark energy is lower than the maximum amount allowed by the big bang nucleosynthesis (BBN) calculation,  $\Omega_{X0} < 0.045$  [21]. We also added blue dashed curves in Fig. 1 to represent the background evolution for  $\epsilon = 10^{-7}$  and  $n = -0.1$ , demonstrating that the energy density of  $X$ -component (here  $F\mu_X$ ) becomes less dominant than the dominant fluids ( $\mu_R$  and  $\mu_M$ ) as  $\epsilon$  gets smaller. The background observables (Hubble parameter and distance modulus) for  $\epsilon < 10^{-3}$  are largely insensitive to  $\epsilon$  and are very similar to those for  $\epsilon = 0.001$ .

In order to calculate the matter and CMB power spectra, we solve a system composed of matter (baryon [ $b$ ] and CDM [ $c$ ]), radiation (photon [ $\gamma$ ] and neutrinos [ $\nu$ ]), and the  $f(R)$  gravity sector as dark energy. The perturbation in the radiation component has been handled by using



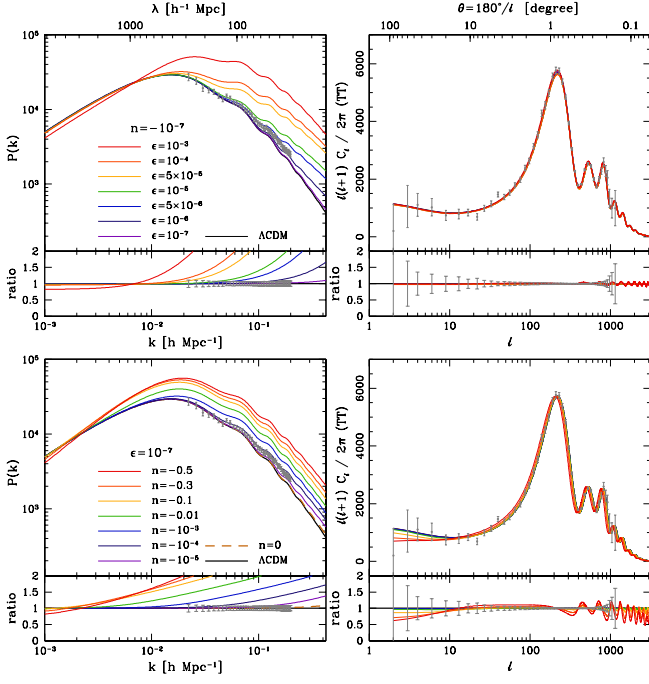


FIG. 2: Top panels: baryonic matter (left) and CMB temperature anisotropy (right) power spectra in the  $f(R) = R^{1+\epsilon} + qR^{-n}$  gravity models with  $n = -10^{-7}$  and varying  $\epsilon = 10^{-7}, 10^{-6}, 5 \times 10^{-6}, 10^{-5}, 5 \times 10^{-5}, 10^{-4}$ , and  $10^{-3}$ . Bottom panels: The same as in the top-panels but with  $\epsilon = 10^{-7}$  and varying  $n = -10^{-5}, -10^{-4}, -10^{-3}, -0.01, -0.1, -0.3$ , and  $-0.5$ . The results for  $\epsilon = 10^{-7}$  and  $n = 0$  are shown as brown dashed curves, which are very similar to the  $\Lambda$ CDM predictions (black curves). In all models including  $\Lambda$ CDM prediction, the same initial amplitude has been assumed. The ratios of  $f(R)$  gravity power spectrum to  $\Lambda$ CDM prediction are also shown in the bottom region of each panel. For matter and CMB power spectra, recent measurement from the Sloan Digital Sky Survey (SDSS) DR7 luminous red galaxies (LRG) [24] and the WMAP 7-year data (including the cosmic variance) [25] have been added (grey dots with error bars) together with fractional errors of observed spectra.

the Boltzmann equation or tight coupling approximation (see Ref. [22] for our set of equations and the numerical methods). As the initial conditions of background and perturbation variables we use Eqs. (14)–(16) and (19) with  $w = \frac{1}{3}$  and  $\Omega_{w0} = \Omega_{R0}$ . All the perturbed variables we use are spatially gauge invariant [23]. We solved the system by adopting the CCG as the temporal gauge condition. The CCG is the same as the synchronous gauge without the gauge mode. For the matter power spectrum we present the power spectrum of baryonic density perturbation based on the CCG which is a gauge-invariant concept. The CMB anisotropy is naturally gauge invariant. Figure 2 shows the matter and CMB temperature anisotropy power spectra for  $n = -10^{-7}$  with varying  $\epsilon$  (top) and for  $\epsilon = 10^{-7}$  with varying  $n$  (bottom panels). We omit CMB polarization power spectra. Note that the baryonic matter power spectra is very sensitive to both

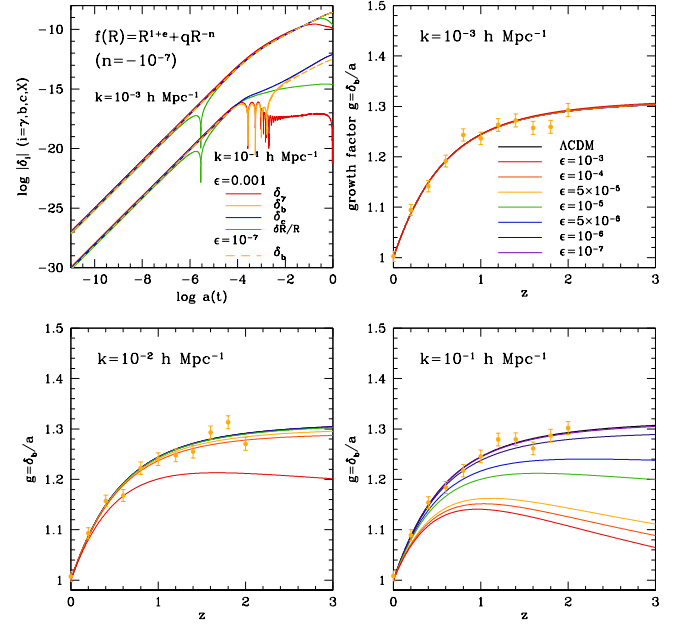


FIG. 3: Top-left: evolution of density perturbations  $\delta_i$  ( $i = \gamma, b, c, X$ ) at comoving scales  $k = 10^{-3}$  and  $10^{-1} h\text{Mpc}^{-1}$  in  $f(R) = R^{1+\epsilon} + qR^{-n}$  gravity with  $n = -10^{-7}$  for  $\epsilon = 0.001$  (solid) and  $\epsilon = 10^{-7}$  (dashed curves). Perturbation growth of photon ( $\gamma$ ), baryon ( $b$ ), CDM ( $c$ ), and  $\delta R/R$  are represented as red, yellow, blue, green curves, respectively. Other panels: evolution of growth factor  $g \equiv \delta_b/a$  (normalized to unity at present) at comoving scales  $k = 10^{-3}, 10^{-2}$ , and  $10^{-1} h\text{Mpc}^{-1}$  for models with parameters used in the top-panels of Fig. 2 ( $n = -10^{-7}$  and varying  $\epsilon$ ) with the same colored code. Growth factors of the  $\Lambda$ CDM model are shown as black curves. Note that since we consider interactions between radiation and baryon components, the  $\Lambda$ CDM growth factor is mildly scale-dependent. Yellow dots with error bars indicate the  $\Lambda$ CDM growth factor expected from the future X-ray and weak-lensing observations [26].

$\epsilon$  and  $n$  while the CMB power spectra (including polarization) are mildly sensitive to the variation of  $n$  and are insensitive to  $\epsilon$ .

Our results for  $\epsilon = 10^{-7}$  and  $n = 0$  (shown as brown dashed curves in the bottom panels of Fig. 2) are very similar to the  $\Lambda$ CDM predictions (black curves); the deviations are less than 2% level at scales  $k < 0.2 h\text{Mpc}^{-1}$  for matter power spectrum and less than 0.5% level for CMB power spectrum. Our calculations of power spectra for  $\epsilon = 10^{-7}$  and nonzero  $n$  are consistent with those presented in Ref. [6] that considered  $f(R) = R + qR^{-n}$  gravity. We have also checked that the power spectra for  $\epsilon = 10^{-7}$  are indistinguishable within the 1% precision from those obtained by evolving the perturbed variables under the model which uses the  $\Lambda$ CDM model in Einstein gravity at the early epoch ( $a/a_0 < 0.001$ ) and suddenly switches to the  $f(R) = R + qR^{-n}$  gravity thereafter.

Figure 3 displays the perturbation growth of individual components ( $\delta_\gamma, \delta_b, \delta_c, \delta R/R$ ) and baryon perturbation growth factor  $g \equiv \delta_b/a$  at recent epoch in our  $f(R)$  grav-

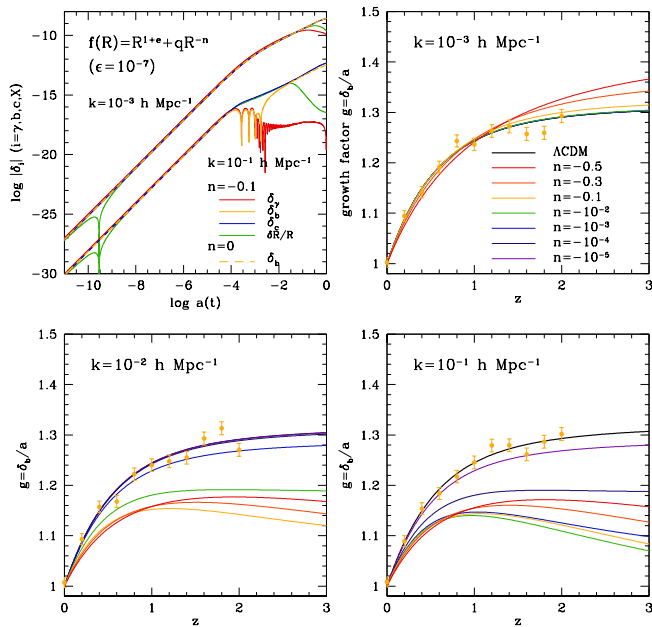


FIG. 4: Same as Fig. 3 but for  $f(R)$  gravity models ( $\epsilon = 10^{-7}$  and varying  $n$ ) used in the bottom-panels of Fig. 2 with the same colored code.

ity with  $n = -10^{-7}$  and varying  $\epsilon$ . We see that each perturbed variable follows with each other at the early epoch, which demonstrates the scaling evolution. In the growth factor panels we have added  $\Lambda$ CDM mock growth factor data points that are expected from the future X-ray and weak-lensing observations [26]. The mock data points, located in the redshift range  $z = 0-2$  with equal interval of  $\Delta z = 0.2$ , have been generated by adding 1% random noise to the  $\Lambda$ CDM growth factor at comoving scales  $k = 0.001, 0.01$ , and  $0.1 \text{ hMpc}^{-1}$ . The perturbation growth factor at the small scale ( $k = 0.1 \text{ hMpc}^{-1}$ ) is very sensitive to the variation of  $\epsilon$ . It is also sensitive to the variation of  $n$ , which is shown in Fig. 4.

From Figs. 2-4 we notice that the CMB power spectrum is less sensitive to the model parameters than the baryon density power spectrum and the baryon growth rate. Thus, in the following we use the baryon density power spectrum and the baryon growth rate together with the SNIa data to constrain the model parameters. Figure 5 shows likelihood distributions of  $f(R)$  gravity parameters constrained by the recent UNION2 SNIa data set (without systematic errors) [20], the SDSS DR7 LRG power spectrum (PS) [24], and the  $\Lambda$ CDM mock growth factor data at the comoving scale  $k = 0.1 \text{ hMpc}^{-1}$  (in the bottom-right panels of Figs. 3 and 4). Our likelihood estimation is tentative since we have explored only the  $\epsilon$ - $n$  space while other cosmological parameters are fixed with the WMAP 7-year best-fit parameters. The likelihood distribution has been calculated from  $L = L_{\max} \exp(-\Delta\chi^2/2)$ , where  $L_{\max}$  has been taken as the maximum value within the parameter space we have explored,  $10^{-8} \leq \epsilon \leq \epsilon_{\text{BBN}}$  and  $-0.5 \leq n \leq -10^{-8}$ .

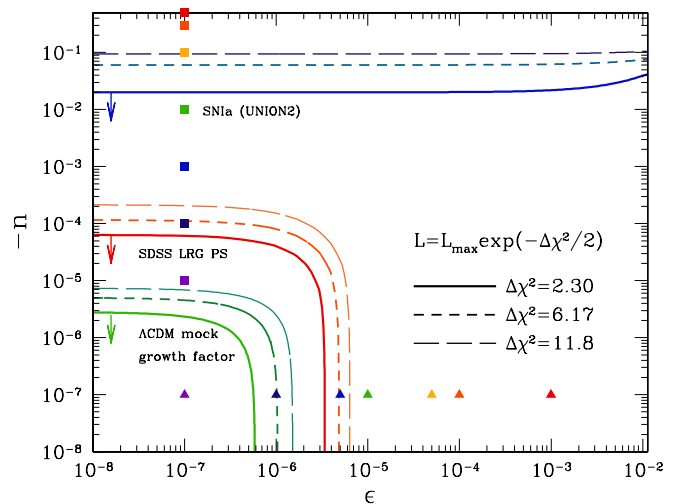


FIG. 5: Likelihood of  $f(R)$  gravity parameters constrained by the UNION2 SNIa sample (blue contours), the SDSS DR7 LRG power spectrum (red contours), and the  $\Lambda$ CDM mock growth factor data at  $k = 0.1 \text{ hMpc}^{-1}$  (green contours). The levels of contours have been determined by setting  $\Delta\chi^2 = 2.30$  (solid), 6.17 (short-dashed), 11.8 (long-dashed curves) relative to the  $\chi^2$ -minimum, mimicking  $1\sigma$ ,  $2\sigma$ ,  $3\sigma$  confidence levels, respectively. Arrows indicate directions to which the likelihood increases. Triangles and squares indicate the models shown in top and bottom panels of Fig. 2 (Fig. 3 and Fig. 4 for the perturbation growth rate), respectively, with the same colored code.

The  $1\sigma$ ,  $2\sigma$ ,  $3\sigma$  confidence levels have been roughly determined by setting  $\Delta\chi^2 = 2.30, 6.17, 11.8$  from the  $\chi^2$ -minimum, which is valid only for the Gaussian distribution. In the  $\chi^2$ -estimation with the SDSS LRG power spectrum, we consider the convolution effect caused by band-power window functions and exclude data points where the non-linear clustering dominates (see Appendix C of Ref. [27] for detailed description). As shown in Fig. 5,  $f(R)$  gravity parameters,  $\epsilon$  and  $n$ , are very sensitive to the growth factor at small scales, and are already tightly constrained by the current measurement of galaxy power spectrum. For  $\Lambda$ CDM mock growth factor data, the likelihood distribution suggests that only the parameter space extremely close to the  $\Lambda$ CDM model is allowed.

## V. DISCUSSION

In this paper we have studied a  $f(R)$ -gravity based dark energy model with early scaling era. We have presented initial conditions of background and perturbed variables during the early scaling evolution regime in the modified gravity with a pure power-law form  $f(R) = R^{1+\epsilon}$  in the early era. With these initial conditions, the modified gravity with a form  $f(R) = R^{1+\epsilon} + f_{\text{DE}}(R)$  where the second term drives the late-time acceleration becomes free from the numerical difficulty that is usually confronted during the background evolution in the

early radiation dominated era for  $f(R) = R + f_{\text{DE}}(R)$  gravity. Our initial conditions are general so that the scaling density evolution of the  $X$ -component is assured for any dominant fluid with a constant equation of state parameter  $w$ .

As a possible dark energy model we have considered the gravity with a form  $f(R) = R^{1+\epsilon} + qR^{-n}$  and compared the evolution of the background and perturbation variables in this gravity with the recent observational data and the  $\Lambda$ CDM mock data. The present observational data already severely constrain our model parameters  $n$  and  $\epsilon$  so that only parameters extremely close to the  $\Lambda$ CDM model is allowed. We found that the power spectrum of baryon component and the perturbation growth factor at small scales are more sensitive to the  $f(R)$  gravity parameters than the SNIa distance mod-

ulus and the CMB anisotropy power spectra (see Figs. 2–5). Therefore, precise measurement of the perturbation growth is essential to tightly constrain our  $f(R)$  gravity.

### Acknowledgments

We thank Dr. Yong-Seon Song for useful discussions. We also wish to thank the anonymous referee for the constructive and helpful comments on our manuscript. H.N. was supported by Mid-career Research Program through National Research Foundation funded by the MEST (No. 2010-0000302). J.H. was supported by the Korea Research Foundation Grant funded by the Korean Government (KRF-2008-341-C00022).

- 
- [1] S. Tsujikawa, arXiv:1004.1493v1; D. Sapone, arXiv:1006.5694.
  - [2] S. Capozziello, V.F. Cardone, S. Carloni, and A. Troisi, *Int. J. Mod. Phys. D* **12**, 1969 (2003); S.M. Carroll, V. Duvvuri, M. Trodden, and M.S. Turner, *Phys. Rev. D* **70**, 043528 (2004); S. Nojiri and S.D. Odintsov, *Phys. Rev. D* **68**, 123512 (2003); A.D. Dolgov and M. Kawasaki, *Phys. Lett. B* **573**, 1 (2003); T. Chiba, *Phys. Lett. B* **575**, 1 (2003).
  - [3] A. de Felice and S. Tsujikawa, *Living Reviews in Relativity*, **13**, 3 (2010); T.P. Sotiriou and V. Faraoni, *Rev. Mod. Phys.* **82**, 451 (2010).
  - [4] L. Amendola, D. Polarski, and S. Tsujikawa, *Int. J. Mod. Phys. D* **16**, 1555 (2007); S.A. Appleby and R.A. Battye, *JCAP* **0805**, 019 (2008); R. Bean, D. Bernat, L. Pogosian, A. Silvestri, and M. Trodden, *Phys. Rev. D* **75**, 064020 (2007); A.W. Brookfield, C. van de Bruck, and L.M.H. Hall, *Phys. Rev. D* **74**, 064028 (2006); S. Capozziello, V.F. Cardone, and A. Troisi, *Phys. Rev. D* **71**, 043503 (2005); S. Capozziello, S. Nojiri, S.D. Odintsov, and A. Troisi, *Phys. Lett. B* **639**, 135 (2006); S. Capozziello and S. Tsujikawa, *Phys. Rev. D* **77**, 107501 (2008); S. Carloni, P.K.S. Dunsby, S. Capozziello, and A. Troisi, *Class. Quant. Grav.* **22**, 4839 (2005); T. Chiba, T.L. Smith, and A.L. Erickcek, *Phys. Rev. D* **75**, 124014 (2007); G. Cognola, E. Elizalde, S. Nojiri, S.D. Odintsov, L. Sebastiani, and S. Zerbini, *Phys. Rev. D* **77**, 046009 (2008); A. Dev, D. Jain, S. Jhingan, S. Nojiri, M. Sami, and I. Thongkool, *Phys. Rev. D* **78**, 083515 (2008); M. Fairbairn and S. Rydbeck, *JCAP* **0712**, 005 (2007); T. Faulkner, M. Tegmark, E.F. Bunn, and Y. Mao, *Phys. Rev. D* **76**, 063505 (2007); S. Fay, S. Nesseris, and L. Perivolaropoulos, *Phys. Rev. D* **76**, 063504 (2007); A.V. Frolov, *Phys. Rev. Lett.* **101**, 061103 (2008); R. Gannouji, B. Moraes, and D. Polarski, *JCAP* **0902**, 034 (2009); Z. Gironés, A. Marchetti, O. Mena, C. Peña-Garay, and N. Rius, arXiv:0912.5474; W. Hu and I. Sawicki, *Phys. Rev. D* **76**, 104043 (2007); E.V. Linder, *Phys. Rev. D* **80**, 123528 (2009); V. Miranda, S.E. Jorás, and I. Waga, *Phys. Rev. Lett.* **102**, 221101 (2009); H. Motohashi, A.A. Starobinsky, and J. Yokoyama, *Prog. Theor. Phys.* **123**, 887 (2010); T. Narikawa and K. Yamamoto, *Phys. Rev. D* **81**, 043528 (2010); I. Navarro and K. Van Acoleyen, *JCAP* **0702**, 022 (2007); S. Nojiri, S.D. Odintsov, *Phys. Lett. B* **657**, 238 (2007); S. Nojiri, S.D. Odintsov, *Phys. Rev. D* **77**, 026007 (2008); G.J. Olmo, *Phys. Rev. D* **72**, 083505 (2005); H. Oyaizu, M. Lima, and W. Hu, *Phys. Rev. D* **78**, 123524 (2008); L. Pogosian and A. Silvestri, *Phys. Rev. D* **77**, 023503 (2008); I. Sawicki and W. Hu, *Phys. Rev. D* **75**, 127502 (2007); F. Schmidt, A. Vikhlinin, and W. Hu, *Phys. Rev. D* **80**, 083505 (2009); Y.S. Song, W. Hu, and I. Sawicki, *Phys. Rev. D* **75**, 044004 (2007); Y.S. Song, H. Peiris, and W. Hu, *Phys. Rev. D* **76**, 063517 (2007); S. Tsujikawa, *Phys. Rev. D* **76**, 023514 (2007); S. Tsujikawa, R. Gannouji, B. Moraes, and D. Polarski, *Phys. Rev. D* **80**, 084044 (2009); S. Tsujikawa, K. Uddin and R. Tavakol, *Phys. Rev. D* **77**, 043007 (2008); K. Yamamoto, G. Nakamura, G. Hütsi, T. Narikawa, and T. Sato, *Phys. Rev. D* **81**, 103517 (2010); P. Zhang, *Phys. Rev. D* **76**, 024007 (2007).
  - [5] L. Amendola, R. Gannouji, D. Polarski, and S. Tsujikawa, *Phys. Rev. D* **75**, 083504 (2007).
  - [6] B. Li and J.D. Barrow, *Phys. Rev. D* **75**, 084010 (2007).
  - [7] L. Amendola and S. Tsujikawa, *Phys. Lett. B* **660**, 125 (2008).
  - [8] W. Hu and I. Sawicki, *Phys. Rev. D* **76**, 064004 (2007).
  - [9] A.A. Starobinsky, *JETP Lett.* **86**, 157 (2007).
  - [10] S.A. Appleby and R.A. Battye, *Phys. Lett. B* **654**, 7 (2007).
  - [11] S. Tsujikawa, *Phys. Rev. D* **77**, 023507 (2008).
  - [12] T. Clifton, *Phys. Rev. D* **78**, 083501 (2008).
  - [13] L. Amendola, D. Polarski, and S. Tsujikawa, *Phys. Rev. Lett.* **98**, 131302 (2007).
  - [14] S. Carloni, P.K.S. Dunsby, and A. Troisi, *Phys. Rev. D* **77**, 024024 (2008).
  - [15] J. Hwang, H. Noh, and C.-G. Park, arXiv:1012.0885.
  - [16] J. Hwang and H. Noh, *Phys. Rev. D* **64**, 103509 (2001).
  - [17] Maplesoft: A Division of Waterloo Maple Inc., <http://www.maplesoft.com>.
  - [18] N. Jarosik, *et al.*, arXiv:1001.4744v1; E. Komatsu, *et al.*, arXiv:1001.4538v2.
  - [19] E. Gaztañaga, A. Cabré, and L. Hui, *Mon. Not. R. Astron. Soc.* **399**, 1663 (2009).

- [20] R. Amanullah, *et al.*, *Astrophys. J.* **716**, 712 (2010).
- [21] R. Bean, S.H. Hansen, and A. Melchiorri, *Phys. Rev. D* **64**, 103508 (2001).
- [22] J. Hwang and H. Noh, *Phys. Rev. D* **65**, 023512 (2002).
- [23] J.M. Bardeen, *Particle Physics and Cosmology*, edited by L. Fang, and A. Zee, (Gordon and Breach, London, 1988), p1; J. Hwang, *Astrophys. J.* **375**, 443 (1991).
- [24] B.A. Reid *et al.*, *Mon. Not. R. Astron. Soc.* **404**, 60 (2010).
- [25] D. Larson *et al.*, arXiv:1001.4635v2.
- [26] A. Vikhlinin, *et al.*, *Astro2010: The Astronomy and Astrophysics Decadal Survey*, Science White Paper, no. 305 [arXiv:0903.5320v1].
- [27] C.-G. Park, J. Hwang, J. Park, and H. Noh, *Phys. Rev. D* **81**, 063532 (2010).
- [28] W.-T. Lin, J.-A. Gu, and P. Chen, arXiv:1009.3488v1.